Polym. Bull. (2010) 64:159–169
DOI 10.1007/s00289-009-0150-z

ORIGINAL PAPER

Graft copolymers of poly(methyl methacrylate) and polyamide-6 via in situ anionic polymerization of ε-caprolactam and their properties

Yao-Chi Liu · Jing-Song Wang · Ke-Long Huang · Wei Xu

Received: 31 January 2009 / Revised: 5 July 2009 / Accepted: 12 August 2009 /

Abstract Graft copolymers of poly(methyl methacrylate) and polyamide-6 (PMMA-g–PA6) were investigated via in situ anionic polymerization of ε-caprolactam, using PMMA precursors with N-carbamated caprolactam pendants (PMMA–CCL) as macroactivators and sodium caprolactamate as catalyst. Three grades of PMMA–CCLs obtained by free radical copolymerization were used for synthesizing the PMMA-g–PA6 copolymers with different PMMA content. The resulting graft copolymer was characterized by Fourier-transform infrared spectroscopy and selective extraction. Scanning electron microscopy is used to clarify the phase morphology of obtained polymer by fracture surface. The thermal property, crystallinity and dimensional stability of graft copolymer were studied using differential scanning calorimetry, X-ray diffraction and water absorption measurement. The results show the T_g of graft copolymer is higher than that of neat PA6, but the onset and peak points of graft copolymer melting point are shifted to lower temperature. The percentage crystallinity and water absorption of PMMA-g–PA6 copolymer decrease with increasing PMMA content, but the crystal structure of PA6 is scarcely affected by the presence of PMMA. Graft copolymers have improved dimensional stabilities relative to neat PA6. Upon the incorporation of 19.9 wt% PMMA into PA6, the water absorption of PMMA-g–PA6 copolymer has been reduced from 4.8 for neat PA6 to 2.1%.

Y.-C. Liu (✉) · K.-L. Huang
Institute of Functional Material Chemistry, School of Chemistry and Chemical Engineering,
Central South University, Changsha 410083, China
e-mail: liuyaochi72@163.com

Y.-C. Liu · J.-S. Wang
School of Urban Construction, University of South China, Hengyang 421001, China

W. Xu
Baling Petrochemical Company, Yueyang 414000, China

Keywords Graft copolymer · Poly(methyl methacrylate) · Polyamide 6 · Anionic polymerization · Properties

Introduction

The approach of blending different polymers has been an explosive growth during the past two decades. The most attractive blends are those in which synergistic behavior can be obtained. Polyamide-6 (PA6, also known as nylon-6) is a crystalline polymer. It has great chemical stability, excellent abrasion resistance and good fatigue; but its affinity to moisture (an equilibrium moisture content of about 6% [1]) makes it difficult to maintain dimensional stability. Poly(methyl methacrylate) (PMMA) is an amorphous polymer with outstanding rigidity, high weatherability, low moisture absorption (0.3–0.4%, 1/8 in bar, 24 h) and high dimensional stability [1]. Blends of these two polymers might show promise for compensating the weakness of the two neat homopolymers.

Hydrolytic and anionic polymerizations of ε-caprolactam (CL) are the most important commercial processes to produce PA6. The former produces a low molecular weight and linear polymer (linear PA6), and the later results in a crosslinked and irregular polymer because of Claisen-type condensations and other side reactions [2, 3]. The binary system of linear PA6 and PMMA has been studied using physically blending [4] and reactive compatibilization [5–7]. These materials exhibit interesting properties such as transparency, creep resistance and solvent resistance. There are, however, no data in the literature about the PMMA/PA6 system via anionic polymerization.

The anionic polymerization of CL is attractive because of its mild reaction requirements, absence of by-product, high degree of conversion and highly crystalline nature [8]. All these advantages make the processes of reactive injection molding (RIM-PA6) and monomer cast (MC-PA6) possible in industrial applications. Based on the anionic polymerization mechanism of CL, an activator is added to the reaction system not only to accelerate polymerization, but also to join the reaction and behave as the starting point of chain growth. Generally the activator has functional group of N-carbamated caprolactam (CCL) in its structure directly or can be formed indirectly. It can be deduced that a polymer containing CCL groups can act as a macroactivator. In this way, PA6 chains will start growing from these groups, and thus a copolymer can be formed through anionic route similar to that for homopolymer PA6 [9, 10].

In our previous investigations [11], PA6 was grafted onto different rigid polymers via in situ anionic polymerization. The preformed rigid polymers with CCL pendants were used as macroactivators of the anionic polymerization of CL. In this work, three grades of PMMA precursors with CCL pendants (PMMA–CCL) were employed for synthesizing the PMMA-g–PA6 copolymers with different PMMA content (Fig. 1). The aim was to study the influence of PMMA content on the thermal property, crystallinity, dimensional stability and water absorption of the obtained PMMA-g–PA6 copolymers via anionic polymerization.

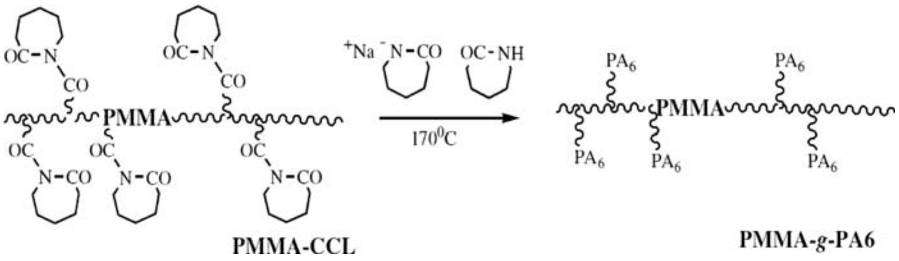

Fig. 1 Mechanism of graft copolymer formation

Experimental

Materials

Methyl methacrylate (MMA) was distilled under reduced pressure to remove the inhibitor before use. 2,2′-azobis(isobutyronitrile) (AIBN) was recrystallized from methanol, and then dried at 60 °C under reduced pressure overnight. CL (China Petr & Chem Co) was recrystallized from acetone (mp: 76–70 °C and bp: 268.5 °C). Toluene, methanol, phosphorus pentoxide (P_2O_5), chloroform ($CHCl_3$), petroleum ether (60–90 °C) and NaOH were used as received. Allyl alcohol ester-based monomer with carbamated caprolactam moiety (ACCL) was synthesized and purified according to Ref. [11]. Yield 82.9%, mp 41.5 °C. PMMA–CCL macroactivators (M1, M2 and M3) were prepared by the free radical copolymerization of MMA and ACCL according to Ref. [11]. AIBN (0.5 mol%) was used as initiator and toluene as solution. The product obtained was precipitated three times in petroleum ether, and then vacuum-dried at 90 °C overnight. Their characteristics are listed in Table 1. For the sake of comparison, pure PMMA was also prepared (M4).

Synthesis of PMMA-g–PA6

Graft copolymers synthesized in this work employed PMMA–CCL as macroactivator and sodium caprolactamate (NaCL) as catalyst (Fig. 1). Polymerization was conducted in a heated oil bath whose temperature was monitored by a thermocouple. Since the anionic polymerization of CL is very sensitive to moisture, all

Table 1 Characteristics of PMMA–CCL and PMMA

Exp	Macroactivator	M_n^{a}, 10^{-4} (g/mol)	PDI^a	CCL^b (mol%)
M1	PMMA–CCL	10.2	2.25	24.8
M2	PMMA–CCL	8.69	2.11	10.1
M3	PMMA–CCL	9.54	2.10	4.96
M4	PMMA	14.7	1.83	–

[a] Measured by GPC in the DMF and LiBr (0.5 mol/L) mixture at 55 °C (universal calibration)

[b] Obtained by FTIR

Table 2 Selected information on the experimental trials carried out in this work

Trial	Composition by molar ratio	R_w[a] (%)	C_m[b] (%)	Y_p[c] (%)	Remark
P0	CL/NaCL/M4 = 100/1/0.5	–	–	–	No polymerization in 2 h
P1	CL/NaCL/ACCL = 100/1/0.5	–	92.1	89.1	Homo-PA6 expected
P2	CL/NaCL/M1 = 100/1/0.5	3.30	90.2	87.0	PMMA-g–PA6 expected
P3	CL/NaCL/M2 = 100/1/0.5	5.51	87.6	83.3	PMMA-g–PA6 expected
P4	CL/NaCL/M3 = 100/1/0.5	9.91	84.4	80.1	PMMA-g–PA6 expected
P5	CL/NaCL/M3 = 100/1/1	19.9	78.9	72.6	PMMA-g–PA6 expected
P6	CL/NaCL/M4/ACCL=100/1/10/0.5	–	89.0	73.5	PMMA/PA6 blend

[a] Weight ration of PMMA–CCL to CL

[b] Monomer conversion calculated by Eq. 1

[c] Polymer yield calculated by Eq. 2

materials were dried thoroughly before use. The selected information of copolymers synthesized in this work was listed in Table 2. In a typical experiment, NaCL component was prepared by the reaction of CL (8.5 g, 75 mmol) and NaOH (60 mg, 1.5 mmol) at 120 °C for 2 h under reduced pressure. Desired amount of PMMA–CCL and CL (8.5 g, 75 mmol) were introduced into an ampoule, and dissolved at 140 °C. Then, NaCL component was poured into the ampoule. The reactant was mixed well in an ultrasonicator at 75 °C for 15 min, and allowed to polymerize at 170 °C for a polymerization time of 30 min.

Selective extraction

Polymers obtained were cut to pieces and grinded in a Thomas Mill at room temperature. Then, the selective Soxhlet extraction consisted in using deionized water and chloroform as extracting solvents was implemented for all samples, and the monomer conversion (C_m) and polymer yield (Y_p) listed in Table 2 were calculated.

$$C_m\,(\%) = \frac{W_2 - W_1}{W_0 - W_1} \times 100 \tag{1}$$

$$Y_p\,(\%) = \frac{W_3}{W_0} \times 100 \tag{2}$$

where W_0 is the weight of dried sample, W_1 is the pro rata weight of macroactivator contained in sample, W_2 is the dried weight of sample left after extracting with hot water for 16 h, and W_3 is the dried weight of sample left after further extracting with hot chloroform for 4 h.

Polymer characterization

Fourier-transform infrared (FT-IR) spectroscopy was preformed on a Nicolet Nexus 670 FT-IR spectroscopy between 4000 and 400 cm^{-1} in the form of KBr pellets.

The morphology of polymers was observed by scanning electron microscopy (SEM) with a Hitachi S4700 microscope. The fracture surfaces of the samples after selective extraction were sputter coated with gold to prevent charging in the electron beam.

Differential scanning calorimetry (DSC) was performed on a Perkin Elmer DSC-7 instrument with a temperature range from 20 to 300 °C and a sample weight of about 7–10 mg under nitrogen atmosphere. Each sample was heated from 20 to 300 °C at a rate of 10 °C min^{-1} before quenching to 20 °C at a rate of 100 °C min^{-1}. Finally, the sample was reheated to 300 °C at a rate of 10 °C min^{-1} at second heating. Crystalline melting temperature (T_m) was obtained as the maximum of the melting endotherm. Percentage crystallinity (χ_{DSC}) of copolymer was calculated via the ratio between the measured and equilibrium heats of fusion ($\Delta H_f/\Delta H_f^0$). The equilibrium heat of fusion (ΔH_f^0) is 230 J g^{-1} for 100% crystalline MCPA6 [10, 12].

X-ray diffraction (XRD) data were performed on a Rigaku D/Max2500 diffractometer (Ni-filtered, Cu/Kα radiation of wavelength 0.154 nm) in the reflection mode over the range of diffraction angles (2θ) from 5° to 45° at ambient temperature. The voltage and tube current were 40 kV and 200 mA, respectively. Percentage crystallinity (χ_{XRD}) was calculated by a standard procedure [13, 14].

Water absorption

To evaluate the dimensional stability of polymers, water absorption measurement was conducted with polymer powders (about 10 g) at ambient temperature for 24 h. Water absorption (W_a) is expressed as increase in weight percent.

$$W_a\,(\%) = \frac{W_5}{W_4} \times 100 \qquad (3)$$

where W_4 is the weight of dried sample after selective extraction, W_5 is the weight of wet sample patted dry with a lint free cloth.

Results and discussion

Polymer synthesis

The mechanism of the formation of graft copolymers is depicted in Fig. 1. PMMA–CCL acts as macroactivator of the anionic polymerization of CL. CL is grafted onto PMMA–CCL backbone to form PMMA-g–PA6 graft copolymers in the presence of catalyst NaCL. The polymerization takes place quickly because of the low activating energy for the initial nucleophilic attack of caprolactam anion on the CCL group [9, 10]. In practice, polymerization phenomena were observed in less than 5 min for **P1**–**P6**, indicating both ACCL and PMMA–CCL own high activating capabilities. The polymerization of **P1** is expected to be a homopolyamide 6 (neat PA6). For the polymerization of **P2**–**P5**, CCL pendants help in functionalizing the PMMA chain. They react with caprolactam anion, and polyamide side chains grow.

Theoretically speaking, the ester group of PMMA can also act as the activator. It can react with NaCL to form CCL groups during the anionic polymerization of CL. But the activating capacity of ester is relatively low. Pae investigated the ability of phenyl ester group to activate the anionic polymerization of CL using phenylmagnesium bromide as catalyst [15]. The time necessary for the polymerization to go to completion is long (4–5 h at 140–150 °C) compared to the mean residence time of a typical monomer cast process (a few minutes). In our work, the polymerization activated by PMMA was not detected in 2 hours (P0) in the presence of catalyst NaCL. When a bit of ACCL was added (**P6**), polymerization phenomenon is similar to **P1**–**P5**. This means the activating capability of CCL group is quite higher than that of methyl ester at this polymerization system. Thus, the product of **P6** is expected to be a simple PMMA/PA6 blend.

Characterization of copolymer

The full characterization of polymer blends remains a challenge. Fractions of grafted species are usually deduced by mass balance after selective extraction of ungrafted chains of each component. This method also allows recovery of pure graft copolymer for further analysis when selective solvents are available. For instance, blends of polyethylene and polyamide were completely characterized using chloroform and formic acid as selective solvents [16]. To our knowledge, there are selective solvents to recover PMMA, but not PA chains, from PMMA/PA mixtures. On the other hand, the polymerization of CL does not result in complete conversion of monomer. Subsequent extracting by hot water is essential to remove unreacted CL monomers and cyclic oligomers from the final product.

In this work, water and chloroform were employed as extracting solvents to evaluate the monomer conversion and polymer yield. The data are listed in Table 2. The monomer conversions of graft copolymers are lower than that of neat PA6. The existence of macroactivators in melting CL hinders the movement of CL and the propagation of PA6 chain, especially at the end of polymerization. In addition, cyclic oligomer contents increase with activator concentration in the anionic polymerization of CL [17]. After successive extraction in water and then in chloroform, those not dissolved correspond to graft copolymers. The polymer yields of graft copolymers are lower than that of neat PA6. As the graft density decreases (from **P2** to **P4**) and the molar ratio of macroactivator/CL increases (**P5**, compared with **P4**), the polymer yield decreases. It is noticeable that some of those products dissolved in chloroform do not necessarily mean that they were not graft copolymers. It could eventually be very rich in PMMA–CCL and very poor in PA6.

The graft copolymer after successive extraction was further characterized by FT-IR. It is known that FT-IR spectroscopy is one of the most established methods for characterizing polyamides. NMR and GPC were unsuitable for this evaluation because of the lack of an appropriate solvent. Figure 2 shows the FT-IR spectra of PMMA–CCL, PMMA-g–PA6 copolymer and neat PA6. The characteristic absorption bands of PMMA–CCL (Fig. 2a) are those corresponding to CCL groups (1711, 1648 and 1595 cm^{-1}). For PMMA-g–PA6 copolymer (Fig. 2b), these absorption bands almost disappear. CCL groups reacted with caprolactam anions to form PA6

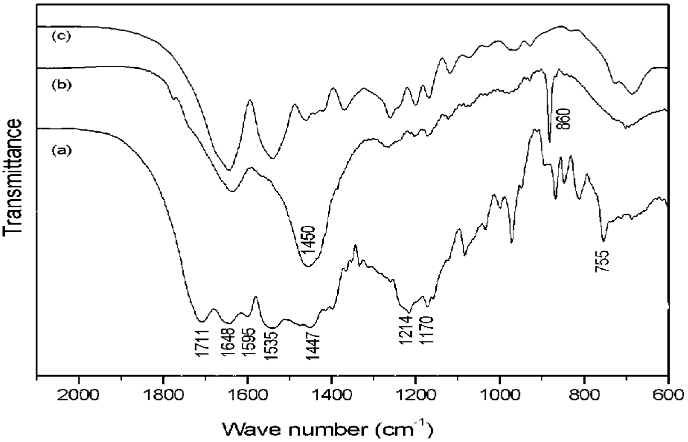

Fig. 2 FT-IR spectra of (a) the PMMA–CCL macroactivator of **M2**, (b) the PMMA-g–PA6 copolymer of **P3**, and (c) neat PA6

chains. Comparing with neat PA6 (Fig. 2c), the graft copolymer shows the strong and characteristic absorption bands of PMMA at 1,450 (C–H deformation of methyl) and 860 cm^{-1} (O=C–O blend). If the final product is not a graft copolymer but a simple PMMA/PA6 blend, PMMA will be extracted from the product, and the characteristic absorption bands of PMMA cannot appear in the FT-IR spectra of the final product.

Morphology of polymers

SEM is a simple method to clarify phase morphology by fracture surfaces. SEM micrographs of neat PA6, PMMA-g–PA6 and PMMA/PA blend are shown in Fig. 3. For the PMMA/PA6 blend (Fig. 3c), spherical holes left by PMMA can be easily observed after selective extraction because of the poor adhesion between the two phases [4]. However, the morphology of graft copolymer (Fig. 3b) is quite homogeneous and a mosaic structure is formed, similar to that of neat PA6 (Fig. 3a). Both the PMMA-g–PA6 copolymer and the PMMA/PA6 blend contain

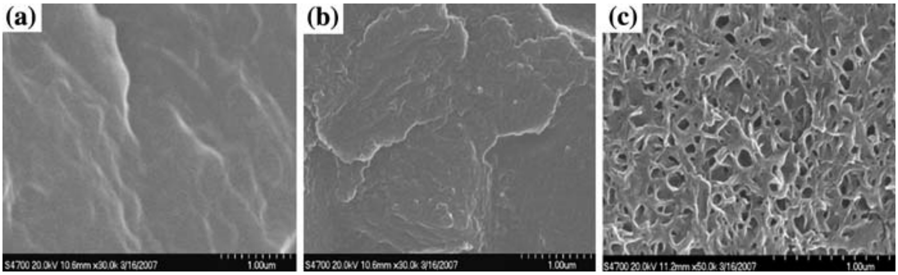

Fig. 3 SEM micrographs of **a** neat PA6, **b** the PMMA-g–PA6 copolymer of **P4**, and **c** the PMMA/PA6 blend of **P6**

Table 3 Thermal property and crystallinity of graft copolymers

Trial	T_g[a] (°C)	T_m[b] (°C)	ΔH_f[c] ($J.g^{-1}$)	χ_{DSC}[d] (%)	χ_{XRD}[e] (%)	W_a[f] (%)
P1	51.0	217.6	57.94	25.19	23.7	4.8
P2	51.8	216.2	55.81	24.27	22.0	4.3
P3	53.1	213.9	51.85	22.54	20.6	3.0
P4	57.5	209.7	49.93	21.71	20.1	2.8
P5	61.7	203.0	47.85	20.80	18.2	2.1

[a] Glass transition temperature, [b] Melting temperature, [c] Heat of fusion, [d] Percentage crystallinity calculated by DSC, [e] Percentage crystallinity calculated by XRD, [f] Water absorption calculated by Eq. 3

two distinctive sequences, they tend not to mix well (immiscible) and usually exhibit two-phase morphology. But the restriction of the covalent bonds between PMMA and PA6 in PMMA-g–PA6 copolymer holds the different blocks together, in this way there is no macroscopic phase separation; segregation only take place at a local scale, i.e. microscopic separation.

Thermal behavior and crystallinity of graft copolymers

Table 3 and Fig. 4 show the thermal properties of polymers determined with DSC. All T_g's of graft copolymers are higher than that of neat PA6. As the PMMA content increases, the magnitude of the increase becomes larger. It is speculated that the increase in T_g is due to the constrained chain mobility in PA6 segments resulting from its chemical attachment to the rigid PMMA backbone. Additionally, PA6 chain flexibility is different due to different molecular weight as PMMA content increases.

The melting behavior of crystalline is described with the crystalline melting temperature (T_m) and the percentage crystallinity (χ_{DSC}) calculated from ΔH_f. The results show both T_m and χ_{DSC} decrease with increasing PMMA content, and the onset melting point of graft copolymer is shifted to lower temperature. The decrease in crystallinity and T_m results from the disruption of polyamide packing due to the presence of PMMA main chains. Well-proportioned PMMA segments are destroyers of the hydrogen bonding of polyamide. The diluent effect becomes more evident at higher PMMA content, and induces forming more PA6 imperfect crystallites, which result in the broadening of melting cure and the depression of melting temperature.

XRD is an alternative method to evaluate the crystallinity of polymers. The percentage crystallinities determined by XRD (χ_{XRD}) are also listed in Table 3 for comparison. There is an excellent agreement between the XRD and DSC estimates of crystallinity for all samples, although the DSC data are shifted to higher values. This good correspondence between the two sets of data supports the general conclusion drawn above.

As regards polymorphism, three XRD powder patterns of the neat PA6, the PMMA/PA6 blend and the graft copolymer P5 are shown in Fig. 5. Neat PA6 (Fig. 5b) shows the α-type crystal structure with two characteristic diffraction peaks

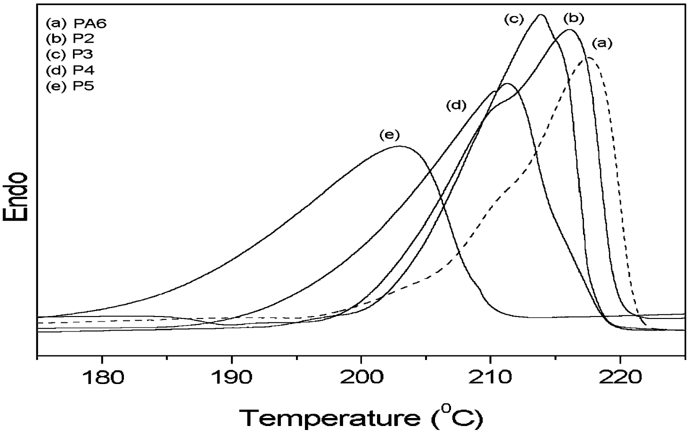

Fig. 4 DSC traces of (a) neat PA6 and the PMMA-g–PA6 graft copolymers of (b) **P2**, (c) **P3**, (d) **P4** and (e) **P5**

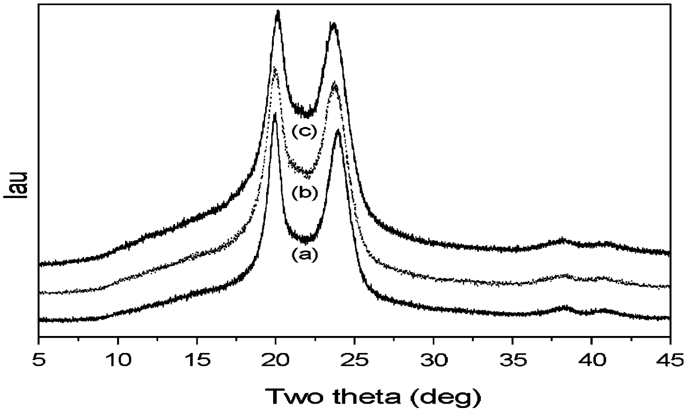

Fig. 5 XRD patterns of (a) PMMA/PA6 blend, (b) neat PA6, and (c) PMMA-g–PA6

at approximately $2\theta = 20.0°$ and 23.8° clearly [18]. After successive extraction in water and then in chloroform, both the blend (Fig. 5a) and the graft copolymer (Fig. 5c) show the same crystal structures as neat PA6. It is a logical expectation for the former since there is a lack of PMMA after selective extraction. The later, however, indicates that in the graft copolymer the crystal structure of PA6 is scarcely affected by the presence of PMMA component.

Dimensional stability of graft copolymers

PA6 is semicrystalline and extremely sensitive to water absorption because of the existence of interchain hydrogen bonding sites between amide groups. This may cause dimensional instability with property degradation and ultimately lead to failure during its life exposure.

The dimensional stability of polyamides could be evaluated by water absorption [19]. The water absorptions of polymers are listed in Table 3. All the graft copolymers have lower moisture absorptions than neat PA6. The water absorption of copolymers decreases with increasing PMMA content. Thus, the moisture resistance of graft copolymer is better than that of neat PA6, and the graft copolymers own higher dimensional stability.

As regards the water absorption mechanism of PMMA-g–PA6 copolymers, two aspects should be taken into account: the percentage crystallinity of PA6 and the hydrophobic nature of PMMA. For neat PA6, as the crystallinity increases the amount of water being absorbed commonly decreases. The water absorption of the PMMA-g–PA6 copolymers obtained in this work, however, does not follow the above rule. As PMMA content increases, a decrease in water absorption follows a decrease in percentage crystallinity. Note that water molecules can only diffuse into the amorphous phase and displace ‘disordered’ amide–amide hydrogen bonds, but they cannot penetrate into the crystal domain and break apart existing amide–amide bonds in this phase [18]. As the initial content of PMMA increases, the proportion of amide groups in amorphous (responsible for water absorption) decreases while that of PMMA segments increases. Thus, the hydrophobic nature of PMMA is experimentally proved to be the main factor in resulting in the decrease of water absorption.

Conclusion

PMMA-g–PA6 copolymers have been obtained by the anionic polymerization of CL in the presence of PMMA–CCL macroactivators. The graft copolymers were characterized by FT-IR and selective extraction. The morphology of graft copolymer is quite homogeneous. As the initial PMMA content increase, the onset and peak points of graft copolymer melting point are shifted to lower temperature; the percentage crystallinity decreases, but the crystal structure of polyamide is not affected by the presence of PMMA component. The graft copolymers show lower water absorption and higher dimensional stability than neat PA6.

Acknowledgements We acknowledge National Natural Science Foundation of China (No. 20707008) and The Postdoctoral Science Foundation of Central South University (No. 69927) for financial support of this research.

References

1. Mark JE (1999) Polymer data handbook. Oxford University Press, New York
2. Crespy D, Landfester K (2005) Anionic polymerization of ε-caprolactam in miniemulsion: synthesis and characterization of polyamide-6 nanoparticles. Macromolecules 38:6882–6887
3. Ricco L, Russo S, Orefice G, Riva F (1999) Anionic poly (ε-caprolactam): Relationships among conditions of synthesis, chain regularity, reticular order, and polymorphism. Macromolecules 32:7726–7731
4. Carone E, Felisberti MI, Nunes SP (1998) Blends of poly(methyl methacrylate) and polyamide. J Mater Sci 33:3729–3735

5. Freluchea M, Iliopoulos I, Millequant M, Flat JJ, Leibler L (2006) Graft copolymers of poly(methyl methacrylate) and polyamide-6: Synthesis by reactive blending and characterization. Macromolecules 39:6905–6912
6. Freluchea M, Iliopoulos I, Flat JJ, Ruzette AV, Leibler L (2005) Self-organized materials and graft copolymers of polymethylmethacrylate and polyamide-6 obtained by reactive blending. Polymer 46:6554–6562
7. Wang X, Li H (2000) Compatiblizing effect of diglycidyl ether of bisphenol-A in polymer blend system: nylon 6 combined with poly(butyle acrylate) core and poly(methyl methacrylate) shell particles. J Appl Polym Sci 77:24–29
8. Udipi K, Dave RS, Kruse RL, Stebbins LR (1997) Polyamides from lactams via anionic ring-opening polymerization 1. Chemistry and some recent findings. Polymer 38:927–938
9. Mateva R, Filyanova R, Velichkova R, Gancheva V (2003) Anionic copolymerization of hexanelactam with functionalized polyisoprene. J Polym Sci Part A 41:487–496
10. Petrov P, Gancheva V, Philipova Tz, Velichkova R, Mateva R (2000) Synthesis of nylon-6 triblock copolymers with bifunctional polymeric activators. J Polym Sci Part A 38:4154–4164
11. Liu Y-C, Xu W, Xiong Y-Q, Zhang F, Xu W-J (2007) An efficient route for the synthesis of graft copolymers with rigid backbones via anionic ring-opening polymerization of caprolactam. Mater Lett 62:1849–1853
12. Boscoletto AB, Trezza G, Andreis B, Milan L, Tavan M, Furlan P (1992) Anionic polyamides modified with poly(oxypropylene) by 'oneshot' RIM technology: structural and morphological characterization. Macromolecules 25:5752–5758
13. Russell DP, Beavmont PW (1980) Structure and properties of injectionmoulded nylon-6. Part 1. Structure and morphology of nylon-6. J Mater Sci 15:197–207
14. Mateva R, Petrov P, Rousseva S, Dimitrov R, Zolova G (2000) On the structure of poly-ε-caprolactams obtained with bifunctional N-carbamyl derivatives of lactams. Eur Polym J 36:813–821
15. Pae Y (2006) Preparation of polyimide/nylon 6 graft copolymers from polyimides containing ester moieties: synthesis and characterization. J Appl Polym Sci 99:309–318
16. van Duin M, Aussems M, Borggreve RJM (1998) Graft formation and chain scission in blends of polyamide-6 and-6,6 with maleic anhydride. J Polym Sci A 36:179–186
17. Ueda K, Hosoda M, Matsuda T, Tai K (1998) Synthesis of high molecular weight nylon 6 by anionrc polymerization of ε-caprolactam. Polym J 30:186–191
18. Rusu G, Ueda K, Rusu E, Rusu M (2001) Polyamides from lactams by centrifugal molding via anionic ring-opening polymerization. Polymer 42:5669–5678
19. Pae Y (2006) Structure and properties of polyimide-g-nylon 6 and nylon 6-b-polyimide-b-nylon 6 copolymers. J Appl Polym Sci 99:300–308